

A SIMPLE PRECONDITIONED DOMAIN DECOMPOSITION METHOD FOR ELECTROMAGNETIC SCATTERING PROBLEMS*

F. Alouges

CMAP, Ecole Polytechnique, Palaiseau, France

Email: alouges@cmapp.polytechnique.fr

J. Bourguignon-Mirebeau

Laboratoire de Mathématiques, Université Paris-Sud XI, Orsay, France

Email: jennifer.mirebeau@gmail.com

D.P. Levadoux

DEMRSFM, ONERA, Palaiseau, France

Email: david.levadoux@onera.fr

Abstract

We present a domain decomposition method (DDM) devoted to the iterative solution of time-harmonic electromagnetic scattering problems, involving large and resonant cavities. This DDM uses the electric field integral equation (EFIE) for the solution of Maxwell problems in both interior and exterior subdomains, and we propose a simple preconditioner for the global method, based on the single layer operator restricted to the fictitious interface between the two subdomains.

Mathematics subject classification: 65F08, 65N38, 65R20.

Key words: Electromagnetism, integral equations methods, Domain decomposition methods, Preconditioning, Cavities.

1. Introduction

Solving scattering Maxwell problems in harmonic regime can be achieved with various methods, among which integral equations (which lead to the so-called boundary element methods) have proven their efficiency. Their main advantage is that they allow to replace a problem posed on the whole space by an equation posed on the surface of the scattering obstacle, reducing a three-dimensional problem to a bi-dimensional one. With the development of such methods, several difficulties arose successively:

- These formulations lead classically to linear systems involving dense matrices (in contrast with finite element methods, for instance). Several methods among which the most famous is probably the FMM (Fast Multipole Method) [28], [29] have been used to circumvent this difficulty.
- There might exist irregular frequencies for which the problem is ill posed [26]. This is typically the case for the so-called EFIE and MFIE formulations. Other types of formulations (e.g., the CFIE) are instead well-posed at any frequency [7].

* Received December 1, 2011 / Revised version received September 16, 2012 / Accepted October 25, 2012 / Published online January 17, 2013 /

- The desire to deal with high frequency problems imposes to use fine discretizations of the equations and consequently to solve large linear systems. This prevents the use of direct solvers, and one usually employs iterative methods. On the one hand, this needs a fast matrix-vector multiplication (which is often realized through the FMM), while on the other hand iterative methods become sensible to the condition number of the system. It has been shown that the underlying systems arising from integral equations are usually badly conditioned and there is a need to develop preconditioning strategies in order to accelerate the convergence of the iterative solver [10,22,30,31]. For instance, the so-called GCSIE methodology has been developed which turns out to be particularly efficient in the case where the object has no cavities and no singularities, by building intrinsically well conditioned integral equations [1, 6, 14, 23, 27].

Nevertheless, when facing realistic problems, one has to treat large objects with complex geometries and new problems are encountered. In this paper, we address the important issue of resonant cavities, motivating the use of a domain decomposition method. Indeed, this is a particularly crucial problem in stealth applications as one needs to take into account the existence of large and resonant cavities, such as air intakes, or cockpits for aircrafts. In classical numerical computations of radar cross sections, these cavities are usually closed in order to avoid the poor convergence of the algorithms [1] giving unrealistic results.

In this paper, we explore a new strategy to deal with this problem. Indeed, we intend to use a domain decomposition method (DDM) in order to split the exterior domain into two subdomains one of which being the cavity. The aim is to decouple the exterior problem (without any cavity) from the problem with boundaries (the cavity itself). This introduces an artificial interface Σ between these subdomains and a new coupling problem posed on Σ (see, Fig. 1.1). For simplicity, we here use on each subdomain the EFIE to solve the corresponding subproblems and to couple the solutions on Σ . This naive DDM algorithm turns out to converge badly. In a latter part we propose a preconditioning technique to accelerate significantly the solution of the DDM.

Historically, the first domain decomposition methods for Helmholtz or Maxwell problems were applied using a finite element method (FEM) in the interior bounded subdomains and a boundary element method (BEM) in the exterior unbounded domain. For instance, Hiptmair considers FEM-BEM methods, first applied to acoustic problems [20] and then to electromagnetic problems [21]. For Helmholtz transmission problems, domain decomposition methods have been used by Balin, Bendali and Collino [4] to specifically treat the case of an electrically deep cavity, and an integral preconditioner using the Calderón formulas has been developed by Antoine and Boubendir [3]. For Maxwell transmission problems, Balin, Bendali and Millot [5] on the one hand, Collino and Millot on the other hand [11,12] propose algebraic preconditioners which use overlapping or nonoverlapping domain decomposition techniques. In iterative domain decomposition techniques, which are split into overlapping and nonoverlapping DDM, the subdomains classically exchange Dirichlet or Neumann data. A substantial improvement using absorbing boundary conditions is made by Desprès [15,16]. The Schwarz method, originally used with Dirichlet or Neumann conditions for overlapping domains, is then adapted by Gander, Halpern and Nataf [19], to nonoverlapping subdomains with more general conditions, of Robin type. The resulting algorithm converges with a high convergence rate for the wave equation in dimension 1. Gander, Halpern and Magoulès [18] optimize the method by taking more general conditions, for the Helmholtz problem in dimension 2. Eventually, Dolean, Gander and Gerardo-Giorda [17] adapt it to obtain a Schwarz optimized method for the harmonic

Maxwell problem in dimension 3.

We present here a nonoverlapping domain decomposition method. This DDM couples the subdomains through the help of an operator, instead of transmitting at each iteration the appropriate conditions from one subdomain to another. We use only integral equations to solve the boundary value problems in the subdomains. In particular, the interior problem is treated with the help of an integral equation, instead of a more classical finite element method. We are not aware of the use of such techniques for solving Maxwell equations with the DDM in the context of integral equations in the literature.

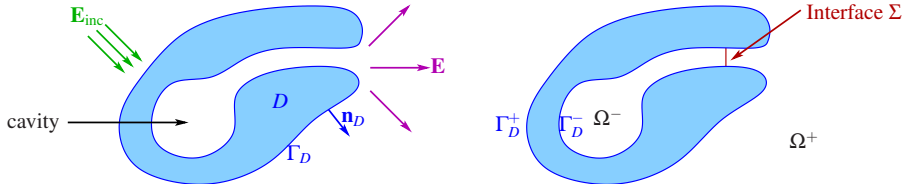


Fig. 1.1. The scattering problem (left) and the decomposition of domain Ω (right).

The paper is organized as follows. The scattering problem is first described and in a second part, we present the domain decomposition method and the condensed problem on the interface. The third part gives a quick overview on classical integral equations methods, and especially of the one we use here, namely the EFIE (Electric Field Integral Equation). The Dirichlet-to-Neumann map of the interface Σ plays a very important role that we describe carefully in the fourth part and this enables us to present a simple analytic preconditioner for the employed DDM, in the fifth part. A validation of the method is presented using pseudo-differential calculus. Eventually, the sixth part gives some numerical results. Substantial improvements are shown validating the approach.

2. The Boundary Value Problem: Assumptions and Notation

We consider a compact set D with a smooth boundary Γ_D . We are particularly interested in the case where the set D contains a large cavity, as illustrated on Fig. 1.1. We assume that the open exterior domain $\Omega = \mathbb{R}^3 \setminus D$ is connected.

Our purpose is to solve the harmonic Maxwell problem when D stands for a scattering metallic object [13, 26]. Waves propagate with constant wave number k in the exterior unbounded domain Ω . The electric field \mathbf{E} is a vector-valued function which satisfies the harmonic Maxwell equation

$$\nabla \times (\nabla \times \mathbf{E}) - k^2 \mathbf{E} = 0 \quad \text{in } \Omega, \quad (2.1)$$

while the related magnetic field is given by

$$\mathbf{H} = \frac{1}{ik} \nabla \times \mathbf{E}. \quad (2.2)$$

An electric field is said to be radiating if it satisfies the well-known Sommerfeld radiation condition

$$\lim_{\|\mathbf{x}\| \rightarrow \infty} \left(\mathbf{x} \times \mathbf{H} + \|\mathbf{x}\| \mathbf{E} \right) = 0. \quad (2.3)$$

Let \mathbf{E}_{inc} be an incident electric field, the electric field \mathbf{E} scattered by the obstacle D is the electric radiating field satisfying the boundary condition $\gamma_D \mathbf{E} = -\gamma_D \mathbf{E}_{\text{inc}}$ on Γ_D , where

$\gamma_D = \mathbf{n}_D \times$ is the metallic trace on Γ_D , \mathbf{n}_D being the unit normal outward to D . In other words, the field \mathbf{E} is solution of the following problem

$$\begin{cases} \nabla \times (\nabla \times \mathbf{E}) - k^2 \mathbf{E} = 0 & \text{in } \Omega, \\ \gamma_D \mathbf{E} = -\gamma_D \mathbf{E}_{\text{inc}} & \text{on } \Gamma_D, \\ \lim_{\|\mathbf{x}\| \rightarrow \infty} \left(\mathbf{x} \times (\nabla \times \mathbf{E}) + ik\|\mathbf{x}\| \mathbf{E} \right) = 0, \end{cases} \quad (2.4)$$

usually named as the perfect electric conductor (PEC) problem.

3. Notation for the Domain Decomposition Method

Domain decomposition methods rely on splitting the computational domain into several subdomains. We present hereafter the application of the method for our case when Ω is decomposed into two subdomains Ω^+ and Ω^- . Namely, we introduce an artificial boundary surface Σ , which splits Ω into an interior bounded domain Ω^- and an exterior unbounded domain Ω^+ (see, Fig. 1.1). We denote by $\Gamma_D^\pm = \Gamma_D \cap \partial\Omega^\pm$, in such a way that the boundary of Ω^\pm is $\Gamma_D^\pm \cup \Sigma$. We call \mathbf{n}^\pm the inward unit normal to Ω^\pm . The notation $\sigma_0^\pm = \mathbf{n}^\pm \times$ and $\sigma_1^\pm = \frac{1}{ik} \mathbf{n}^\pm \times (\nabla \times)$ stand for the classical electric and magnetic traces on Σ .

We introduce the short-cut field \mathbf{E}_{sc} , which is the radiating electric field defined on Ω^+ , having a tangential trace on $\Gamma_D^+ \cup \Sigma$, and such that $\gamma_D \mathbf{E}_{\text{sc}} = -\gamma_D \mathbf{E}_{\text{inc}}$ on Γ_D^+ and $\sigma_0^+ \mathbf{E}_{\text{sc}} = -\sigma_0^+ \mathbf{E}_{\text{inc}}$ on Σ (see, Fig. 3.1). In other words, \mathbf{E}_{sc} is the field scattered by the object when interface Σ becomes metallic.

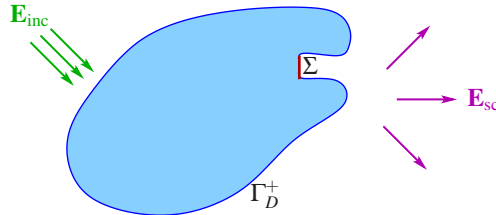


Fig. 3.1. Short-cut field \mathbf{E}_{sc} .

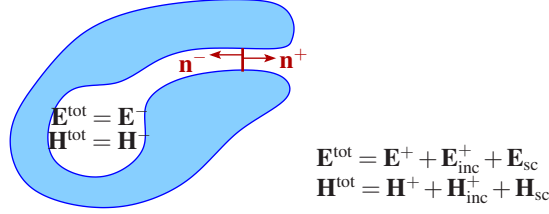
We denote by $\mathbf{E}_{\text{inc}}^\pm$ the restriction of the incident field \mathbf{E}_{inc} to the domain Ω^\pm . We look for the scattered field solution of the PEC problem (2.4) under the form $\mathbf{E}^- - \mathbf{E}_{\text{inc}}^-$ inside Ω^- and $\mathbf{E}^+ + \mathbf{E}_{\text{sc}}$ inside Ω^+ , where \mathbf{E}^+ and \mathbf{E}^- respectively belong to spaces of *admissible* waves W^+ and W^- .

More precisely, the space W^- is the set of all electric fields \mathbf{E}^- which are defined on Ω^- , have a tangential trace on $\Gamma_D^- \cup \Sigma$, and satisfy $\gamma_D \mathbf{E}^- = 0$ on Γ_D^- . Correspondingly, W^+ is the space of all *radiating* electric fields \mathbf{E}^+ which are defined on Ω^+ , have a tangential trace on $\Gamma_D^+ \cup \Sigma$, and satisfy $\gamma_D \mathbf{E}^+ = 0$ on Γ_D^+ . Since the subdomain Ω^- is bounded, the radiation condition is not required for the fields in W^- .

The total electric fields therefore have the expression

$$\mathbf{E}^{\text{tot}} = \begin{cases} \mathbf{E}^- & \text{in } \Omega^-, \\ \mathbf{E}^+ + \mathbf{E}_{\text{inc}}^+ + \mathbf{E}_{\text{sc}} & \text{in } \Omega^+, \end{cases}$$

whereas the total magnetic fields (computed from the electric fields with (2.2)) have the ex-

Fig. 3.2. Total fields \mathbf{E}^{tot} and \mathbf{H}^{tot} .

pression

$$\mathbf{H}^{\text{tot}} = \begin{cases} \mathbf{H}^- & \text{in } \Omega^-, \\ \mathbf{H}^+ + \mathbf{H}_{\text{inc}}^+ + \mathbf{H}_{\text{sc}} & \text{in } \Omega^+. \end{cases}$$

Since Σ is an artificial boundary, the total fields \mathbf{E}^{tot} and \mathbf{H}^{tot} are continuous across Σ , and the problem (2.4) becomes the transmission problem

$$\text{Find } (\mathbf{E}^+, \mathbf{E}^-) \in (W^+, W^-), \quad \begin{cases} \mathbf{n}^+ \times \mathbf{E}^- = \mathbf{n}^+ \times (\mathbf{E}^+ + \mathbf{E}_{\text{inc}}^+ + \mathbf{E}_{\text{sc}}), \\ \mathbf{n}^+ \times \mathbf{H}^- = \mathbf{n}^+ \times (\mathbf{H}^+ + \mathbf{H}_{\text{inc}}^+ + \mathbf{H}_{\text{sc}}), \end{cases} \quad \text{on } \Sigma. \quad (3.1)$$

Notice that by construction the short-cut field \mathbf{E}_{sc} verifies $\mathbf{n}^+ \times \mathbf{E}_{\text{inc}}^+ + \mathbf{n}^+ \times \mathbf{E}_{\text{sc}} = 0$ on Σ , and thus, defining the right hand side current

$$\mathbf{u}_{\text{rhs}} = \mathbf{n}^+ \times \mathbf{H}_{\text{inc}}^+ + \mathbf{n}^+ \times \mathbf{H}_{\text{sc}} \quad \text{on } \Sigma,$$

equation (3.1) rewrites as

$$\begin{cases} \mathbf{E}_{\text{tan}}^- = \mathbf{E}_{\text{tan}}^+, \\ -\mathbf{n}^- \times \mathbf{H}^- = \mathbf{n}^+ \times \mathbf{H}^+ + \mathbf{u}_{\text{rhs}}, \end{cases} \quad \text{on } \Sigma. \quad (3.2)$$

The preceding system, which expresses the DDM, will be solved using integral equations inside each subdomain. We recall these integral equations methods in the next section.

4. Integral Equations

Integral equations methods are commonly used to solve electromagnetic scattering problems. We hereafter give a short overview of the construction of these methods. We first recall the definitions of the single and double layer potentials, as well as the fundamental Stratton-Chu formula, before describing the principle of those integral equations.

Let D_0 be a compact and connected subset of \mathbb{R}^3 with a smooth boundary Γ_0 , defining two open and connected domains, the interior bounded domain Ω_0^- and the exterior unbounded domain Ω_0^+ . We denote by \mathbf{n} the unit outward normal to Γ_0 and by γ_T the tangential trace on Γ_0 from domain Ω_0^+ . The PEC problem can be formulated as follows: find the electric radiating field \mathbf{E} defined on Ω_0^+ and satisfying the boundary condition $\gamma \mathbf{E} = \mathbf{u}_0$, where $\gamma = \mathbf{n} \times \gamma_T$ is a trace on Γ_0 , and $\mathbf{u}_0 = -\mathbf{n} \times \mathbf{E}_{\text{inc}}$ is a given current depending on an incident field.

The classical vector potential \mathcal{G} maps a tangential vector-field $\mathbf{u} \in \mathcal{D}'_T(\Gamma_0)$ to the vector-field defined on Ω_0^+ and Ω_0^- by

$$\mathcal{G}\mathbf{u}(x) = -\frac{1}{4\pi} \int_{\Gamma_0} \frac{e^{ik\|x-y\|}}{\|x-y\|} \mathbf{u}(y) dy, \quad (4.1)$$

where $\|\cdot\|$ denotes the euclidean norm on \mathbb{R}^3 . Then we define the single layer potential \mathcal{T} and the double layer potential \mathcal{K} by

$$\mathcal{T} = \frac{1}{ik} \nabla \times (\nabla \times \mathcal{G}) \quad \text{and} \quad \mathcal{K} = \nabla \times \mathcal{G}. \quad (4.2)$$

The electromagnetic potentials satisfy the following important property: given a current \mathbf{u} on Γ_0 , the fields $\mathcal{T}\mathbf{u}$ and $\mathcal{K}\mathbf{u}$ are automatically solutions of Maxwell equation (2.1) and the radiation condition (2.3), [26]. The boundary operators \mathbf{T} and \mathbf{K} are obtained from the electromagnetic potentials and are defined by

$$\mathbf{n} \times \mathbf{T} = \mathbf{n} \times \gamma_T(\mathcal{T}) \quad \text{and} \quad \mathbf{n} \times \mathbf{K} = \mathbf{n} \times \gamma_T(\mathcal{K}) + \text{Id}/2. \quad (4.3)$$

It turns out that \mathbf{T} and \mathbf{K} are pseudo-differential operators respectively of order $+1$ and -1 , see, e.g., [9, 13, 26].

The Stratton-Chu formulas [13], [26] use the single and double layer potentials to express an electric radiating field \mathbf{E} and the related magnetic field \mathbf{H} in terms of their boundary traces.

$$\mathbf{E} = \mathcal{T}(\mathbf{n} \times \mathbf{H}) - \mathcal{K}(\mathbf{n} \times \mathbf{E}) \quad \text{and} \quad \mathbf{H} = -\mathcal{K}(\mathbf{n} \times \mathbf{H}) - \mathcal{T}(\mathbf{n} \times \mathbf{E}). \quad (4.4)$$

These formulas, also known as representation theorem, are the foundation of integral equations, as we shall see now.

The incident field does not satisfy the radiation condition and therefore the representation theorem (4.4) does not apply to \mathbf{E}_{inc} and \mathbf{H}_{inc} . Instead, because \mathbf{E}_{inc} and \mathbf{H}_{inc} are continuous on the whole space \mathbb{R}^3 , their traces have no jump across Γ_0 and one can show that

$$0 = \mathcal{T}(\mathbf{n} \times \mathbf{H}_{\text{inc}}) - \mathcal{K}(\mathbf{n} \times \mathbf{E}_{\text{inc}}) \quad \text{and} \quad 0 = -\mathcal{K}(\mathbf{n} \times \mathbf{H}_{\text{inc}}) - \mathcal{T}(\mathbf{n} \times \mathbf{E}_{\text{inc}}). \quad (4.5)$$

Summing up (4.4) and (4.5), combined with the PEC boundary condition, we obtain the EFIE and MFIE equations,

$$\text{EFIE} : \mathbf{T}\mathbf{u} = -\mathbf{E}_{\text{inc}}^{\text{tan}}, \quad \text{MFIE} : \left(\mathbf{n} \times \mathbf{K} + \frac{1}{2}\text{Id} \right) \mathbf{u} = \mathbf{n} \times \mathbf{H}_{\text{inc}}, \quad (4.6)$$

where $\mathbf{E}_{\text{inc}}^{\text{tan}}$ is the tangential component of \mathbf{E}_{inc} and the unknown \mathbf{u} is equal to $\mathbf{n} \times \gamma_T(\mathbf{H} + \mathbf{H}_{\text{inc}})$.

Unfortunately, the EFIE and the MFIE are well-known to be ill posed at resonant frequencies [26]. Their linear combination, weighted by an arbitrary parameter $\alpha \in]0, 1[$, yields the CFIE, which instead is well posed at any frequency [7], [24],

$$\text{CFIE} : (1 - \alpha)\mathbf{T}\mathbf{u} + \alpha \left(\mathbf{n} \times \mathbf{K} + \frac{1}{2}\text{Id} \right) \mathbf{u} = -(1 - \alpha)\mathbf{E}_{\text{inc}}^{\text{tan}} + \alpha \mathbf{n} \times \mathbf{H}_{\text{inc}}. \quad (4.7)$$

In what follows and for the sake of simplicity, since we are mainly interested in the interface problem on Σ , we only concentrate on the EFIE for solving the electromagnetic problems inside the subdomains.

5. Admittance Operators and the DDM

The structure of the problem (3.2) naturally leads to introduce the so-called admittance operators¹⁾ on Σ

$$\mathbb{A}_{\Sigma}^{\pm} : \mathbf{E}_{\text{tan}}^{\pm} \mapsto \mathbf{n}^{\pm} \times \mathbf{H}^{\pm},$$

¹⁾ Such operators are also classically called Dirichlet-to-Neumann or Steklov-Poincaré operators.

where $\mathbf{H}^\pm = \frac{1}{ik} \nabla \times \mathbf{E}^\pm$, and $\mathbf{E}^\pm \in W^\pm$ solves $\gamma_T \mathbf{E}^\pm = \mathbf{E}_{\text{tan}}^\pm$. Notice that although the input and output data of \mathbb{A}_Σ^\pm are defined only on Σ , the admittance operators are highly non-local and depend on the whole geometry of the domains Ω^\pm .

We remark that

$$\mathbb{A}_\Sigma^\pm = R^\pm \mathbb{A}^\pm P^\pm,$$

where $P^\pm : \mathcal{D}'(\Sigma) \rightarrow \mathcal{D}'(\Gamma_D^\pm \cup \Sigma)$ extends by 0, on $\partial\Omega^\pm$, data defined on Σ , while conversely, $R^\pm : \mathcal{D}'(\Gamma_D^\pm \cup \Sigma) \rightarrow \mathcal{D}'(\Sigma)$ restricts to Σ data defined on $\partial\Omega^\pm$. Here \mathbb{A}^\pm are the admittance operators of $\partial\Omega^\pm$ which map currents $\mathbf{E}_{\text{tan}}^\pm$ defined on the whole *closed* boundaries $\partial\Omega^\pm$ to their magnetic traces $\mathbf{n}^\pm \times \mathbf{H}^\pm$.

The system (3.2) can then be expressed in terms of the admittance operators \mathbb{A}_Σ^\pm

$$\begin{cases} \mathbf{E}_{\text{tan}}^- = \mathbf{E}_{\text{tan}}^+, \\ -\mathbb{A}_\Sigma^- \mathbf{E}_{\text{tan}}^- = \mathbb{A}_\Sigma^+ \mathbf{E}_{\text{tan}}^+ + \mathbf{u}_{\text{rhs}}, \end{cases} \quad (5.1)$$

which eventually reduces to

$$(\mathbb{A}_\Sigma^+ + \mathbb{A}_\Sigma^-) \mathbf{E}_{\text{tan}} = -\mathbf{u}_{\text{rhs}}, \quad (5.2)$$

with $\mathbf{E}_{\text{tan}} = \mathbf{E}_{\text{tan}}^+ = \mathbf{E}_{\text{tan}}^-$.

Equation (5.2) is at the heart of our domain decomposition method. We explain below how the admittance operators \mathbb{A}_Σ^+ and \mathbb{A}_Σ^- are numerically computed, while Section 6 is devoted to the preconditioning of the subsequent linear system.

The admittance operators \mathbb{A}_Σ^\pm can be naturally obtained by solving an integral equation, which involves four electromagnetic potentials described below. The main difference between our particular case and the classical theory is that the domains Ω^+ and Ω^- are *not complementary one to another*. The boundaries of these domains are therefore distinct, although they share the same interface Σ . Consequently, the convolution operators with the Green kernel related to the exterior and the interior electromagnetic potentials, that we next introduce, are not defined on the same surfaces.

Similarly to the potential \mathcal{G} defined by (4.1), we define the vector potentials \mathcal{G}^\pm which map tangential vector-fields $\mathbf{u}^\pm \in \mathcal{D}'_T(\Gamma_D^\pm \cup \Sigma)$ to the vector-fields defined on Ω^\pm by

$$\mathcal{G}^\pm \mathbf{u}^\pm(x) = -\frac{1}{4\pi} \int_{\Gamma_D^\pm \cup \Sigma} \frac{e^{ik\|x-y\|}}{\|x-y\|} \mathbf{u}^\pm(y) dy.$$

As before, the potentials \mathcal{G}^\pm are used to define the single layer potentials \mathcal{T}^\pm and the double layer potentials \mathcal{K}^\pm as follows,

$$\mathcal{T}^\pm = \frac{1}{ik} \nabla \times (\nabla \times \mathcal{G}^\pm) \quad \text{and} \quad \mathcal{K}^\pm = \nabla \times \mathcal{G}^\pm,$$

while

$$\mathbf{n}^\pm \times \mathcal{T}^\pm = \mathbf{n}^\pm \times \gamma_T^\pm(\mathcal{T}^\pm) \quad \text{and} \quad \mathbf{n}^\pm \times \mathcal{K}^\pm = \mathbf{n}^\pm \times \gamma_T^\pm(\mathcal{K}^\pm) + \text{Id}/2,$$

where γ_T^\pm stand for the tangential traces on $\partial\Omega^+$ and $\partial\Omega^-$. As previously, as long as the boundaries $\Gamma_D^\pm \cup \Sigma$ are smooth, pseudo-differential operators \mathbb{T}^\pm and \mathbb{K}^\pm are of order +1 and -1 respectively.

Given an electric field $\mathbf{E}^\pm \in W^\pm$ and its magnetic counterpart \mathbf{H}^\pm , we define the following electromagnetic traces on the boundary $\Gamma_D^\pm \cup \Sigma$,

$$\sigma_0^\pm \mathbf{E}^\pm = \mathbf{n}^\pm \times \mathbf{E}^\pm \quad \text{and} \quad \sigma_1^\pm \mathbf{E}^\pm = \mathbf{n}^\pm \times \mathbf{H}^\pm \quad \text{on} \quad \partial\Omega^\pm = \Gamma_D^\pm \cup \Sigma. \quad (5.3)$$

Using the representation theorem (4.4) in the domain Ω^\pm , we obtain the expression of any electric field \mathbf{E}^\pm in W^\pm in terms of its boundary traces on $\Gamma_D^\pm \cup \Sigma$.

$$\forall \mathbf{E}^\pm \in W^\pm, \quad \mathbf{E}^\pm = \mathcal{T}^\pm(\sigma_1^\pm \mathbf{E}^\pm) - \mathcal{K}^\pm(\sigma_0^\pm \mathbf{E}^\pm). \quad (5.4)$$

Now, for a current $\mathbf{u}_0^\pm \in \mathcal{D}'_T(\Sigma)$ defined on the fictitious interface Σ , we have

$$\mathbb{A}_\Sigma^\pm \mathbf{u}_0^\pm = \sigma_1^\pm(\mathbf{E}^\pm),$$

where $\mathbf{E}^\pm \in W^\pm$ is such that $\mathbf{E}_{\text{tan}}^\pm = P^\pm \mathbf{u}_0^\pm$. Several integral formulations can be used to compute effectively $\mathbb{A}_\Sigma^\pm \mathbf{u}_0^\pm$. As an example, we shall see hereafter that $\mathbb{A}_\Sigma^\pm \mathbf{u}_0^\pm = R^\pm \mathbf{u}^\pm$ where $\mathbf{T}^\pm(\mathbf{u}^\pm) = \left(\frac{1}{2}\text{Id} + \mathbf{K}^\pm \mathbf{n}^\pm \times\right) (P^\pm \mathbf{u}_0^\pm)$.

Indeed, restricting ourselves to the exterior subdomain, our first goal is to find $\mathbf{E}^+ \in W^+$ such that $\mathbf{E}_{\text{tan}}^+ = P^+ \mathbf{u}_0^+$. Applying the trace σ_0^+ to the Stratton-Chu formula (5.4) leads to

$$(\mathbf{n}^+ \times \mathbf{T}^+)(\sigma_1^+ \mathbf{E}^+) = \left(\frac{1}{2}\text{Id} + \mathbf{n}^+ \times \mathbf{K}^+\right) (\sigma_0^+ \mathbf{E}^+) \quad \text{on } \partial\Omega^+.$$

Taking the cross product of the previous equation with $-\mathbf{n}^+$ yields

$$\mathbf{T}^+(\mathbf{n}^+ \times \mathbf{H}^+) = \left(\frac{1}{2}\text{Id} + \mathbf{K}^+ \mathbf{n}^+ \times\right) (\mathbf{E}_{\text{tan}}^+) \quad \text{on } \partial\Omega^+.$$

This problem has the form of an electric field integral equation (EFIE):

$$\text{Find the current } \mathbf{u}^+, \text{ such that } \quad \mathbf{T}^+(\mathbf{u}^+) = \left(\frac{1}{2}\text{Id} + \mathbf{K}^+ \mathbf{n}^+ \times\right) (P^+ \mathbf{u}_0^+) \quad \text{on } \partial\Omega^+. \quad (5.5)$$

The restriction to Σ of the solution \mathbf{u}^+ of (5.5) is the trace $\mathbf{n}^+ \times \mathbf{H}^+$ we look for, and we therefore have

$$\mathbb{A}_\Sigma^+ \mathbf{u}_0^+ = R^+ \mathbf{u}^+,$$

as claimed.

The cavity (Ω^-) is treated similarly, with the restriction that \mathbb{A}_Σ^- is well defined. This is the case when k^2 is not an eigenvalue for the interior Maxwell problem.

Remark 5.1. Since this method is based on an EFIE formulation, it applies to the computation of the admittance \mathbb{A}_Σ^\pm in both subdomains, but with the following *caveat*: metallic problems having irregular frequencies ([13.26]) the EFIE is ill-posed at frequencies close to these resonances. Despite this drawback, the EFIE is still widely used for it is one of the methods which give the most accurate results.

6. Preconditioning the DDM

As we shall see in Section 7, the equation (5.2) unfortunately leads after discretization to an ill-conditioned linear system. We therefore propose a simple preconditioner in order to obtain a tractable DDM which improves the convergence rate.

The purpose of this section is to introduce a theoretical framework which suggests that the preconditioned equation is well posed. Unfortunately, these theoretical results only apply so far in an ideal setting which is not satisfied in practical situations. They should therefore be regarded as a heuristic and hopefully as the foundation of future more general results.

6.1. A preliminary lemma

Let D_0 be a compact subset of \mathbb{R}^3 with a smooth boundary Γ_0 , defining two open domains : the interior domain Ω_0^- (the interior of D_0) and the exterior domain $\Omega_0^+ = \mathbb{R}^3 \setminus D_0$. We define as before the admittance operators related to the boundary Γ_0 , \mathbb{A}_0^- for the interior domain and \mathbb{A}_0^+ for the exterior domain. Also, the single layer potential \mathcal{T} and its tangential trace T are respectively given by (4.2) and (4.3) for the boundary Γ_0 .

The idea for preconditioning our method is based on the following lemma.

Lemma 6.1. *If k^2 is not an eigenvalue for the interior Maxwell problem, then \mathbb{A}_0^- is well defined and we have*

$$(\mathbb{A}_0^+ + \mathbb{A}_0^-)T = \text{Id}, \quad (6.1)$$

$$T(\mathbb{A}_0^+ + \mathbb{A}_0^-) = \text{Id}. \quad (6.2)$$

Proof. Let $\mathbf{u} \in \mathcal{D}'_T(\Gamma_0)$ be a current on Γ_0 . We define $\mathbf{E} = \mathcal{T}\mathbf{u}$ on Ω^+ and Ω^- . Then by continuity of the potential \mathcal{T} across Γ_0 ,

$$\mathbf{E}_{\text{tan}}^+ = \mathbf{E}_{\text{tan}}^- = T\mathbf{u}.$$

Thus

$$\begin{aligned} \mathbf{n}^+ \times \mathbf{H}^+ + \mathbf{n}^- \times \mathbf{H}^- &= \mathbb{A}_0^+ \mathbf{E}_{\text{tan}}^+ + \mathbb{A}_0^- \mathbf{E}_{\text{tan}}^- = (\mathbb{A}_0^+ + \mathbb{A}_0^-)(T\mathbf{u}) \\ &= (\sigma_1^+ \mathcal{T} - \sigma_1^- \mathcal{T})\mathbf{u} = \mathbf{u}, \end{aligned}$$

since the Neumann gap of the single layer potential is the identity [26]. We recall that σ_1^\pm is the electromagnetic trace defined in (5.3). We have proven (6.1).

For (6.2), since k^2 is not an eigenvalue for the interior Maxwell problem, the operator T is bijective and there exists $\mathbf{v} \in \mathcal{D}'_T(\Gamma_0)$ such that $\mathbf{u} = T\mathbf{v}$. Defining $\mathbf{E} = \mathcal{T}\mathbf{v}$ on Ω^+ and Ω^- leads to

$$\mathbf{E}_{\text{tan}}^+ = \mathbf{E}_{\text{tan}}^- = T\mathbf{v} = \mathbf{u}.$$

Consequently,

$$T(\mathbb{A}_0^+ + \mathbb{A}_0^-)\mathbf{u} = T(\sigma_1^+ - \sigma_1^-)\mathcal{T}\mathbf{v} = T\mathbf{v} = \mathbf{u},$$

since the Neumann gap of the single layer potential is the identity. \square

This lemma suggests to precondition the equation (5.2) by the operator T_Σ defined by the operator T restricted to the interface Σ .

Definition 6.1 (Operator T_Σ) *We denote by F the explicit kernel of the single layer potential \mathcal{T} , which can be computed from (4.1) and (4.2). The operator $T_\Sigma : \mathcal{D}'_T(\Sigma) \rightarrow \mathcal{D}'_T(\Sigma)$ is defined as the convolution operator, restricted to Σ*

$$T_\Sigma \mathbf{u}(x) = \int_\Sigma F(x-y)\mathbf{u}(y) dy.$$

Notice that T_Σ does not depend on Γ_D^\pm .

6.2. A preconditioner for the DDM

We aim at proving that the operators $T_\Sigma(\mathbb{A}_\Sigma^+ + \mathbb{A}_\Sigma^-)$ and $(\mathbb{A}_\Sigma^+ + \mathbb{A}_\Sigma^-)T_\Sigma$ are compact perturbations of the identity, using arguments of pseudo-differential theory. This unfortunately restricts our results to smooth boundaries $\partial\Omega^\pm$ which in turn implies that $\partial\Omega$ is not smooth in general (see, Fig. 1.1).

Therefore, we consider a simplified setting in which we assume that the boundary Γ_D is not smooth but such that both boundaries $\Gamma_D^+ \cup \Sigma$ and $\Gamma_D^- \cup \Sigma$ are of C^∞ regularity. For instance, in dimension 2, this implies the existence of two cusps (Fig. 6.1, on the left).

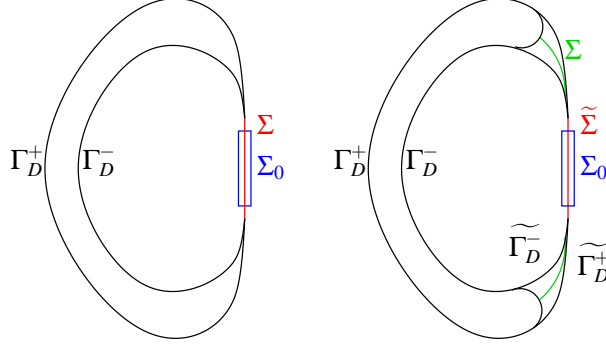


Fig. 6.1. The setting for the theorem (left) and the real case (right).

Let Σ_0 be a compact subset of Σ , and let $\chi_0 : \Sigma \rightarrow [0, 1]$ be a C^∞ cut-off function, supported in the interior of Σ , and such that $\chi_0 = 1$ on Σ_0 . We denote by $T_\Sigma = R^\pm T^\pm P^\pm$ and by \widetilde{T}_Σ the operator

$$\widetilde{T}_\Sigma = \chi_0 T_\Sigma. \quad (6.3)$$

We prove that \widetilde{T}_Σ is a good *left* preconditioner when applied to functions supported on Σ_0 .

Theorem 6.1 (A preconditioner for the DDM) *Let $\mathbf{H}_{T,0}^s(\Sigma) = \{\mathbf{u} \in \mathbf{H}_T^s(\Sigma), \text{ such that } \mathbf{u} = 0 \text{ on } \Sigma \setminus \Sigma_0\}$. For all $\mathbf{u} \in \mathbf{H}_{T,0}^s(\Sigma)$, we have*

$$\widetilde{T}_\Sigma(\mathbb{A}_\Sigma^+ + \mathbb{A}_\Sigma^-)\mathbf{u} = \mathbf{u} + \mathbf{v}, \quad (6.4)$$

where $\mathbf{v} \in \mathbf{H}_T^{s+1}(\Sigma)$. More precisely, $\widetilde{T}_\Sigma(\mathbb{A}_\Sigma^+ + \mathbb{A}_\Sigma^-)$ is a compact perturbation of the identity in $\mathbf{H}_{T,0}^s(\Sigma)$.

Proof. The representation theorem (5.4) applied to the smooth boundary $\Gamma_D^+ \cup \Sigma$ yields

$$(\mathbf{n}^+ \times \mathbf{T}^+)(-\mathbb{A}^+ \mathbf{n}^+ \times) - \left(\mathbf{n}^+ \times \mathbf{K}^+ - \frac{1}{2} \text{Id} \right) = \text{Id}.$$

Therefore,

$$\mathbf{T}^+ \mathbb{A}^+ = \frac{1}{2} \text{Id} + \mathbf{K}^+ \mathbf{n}^+ \times. \quad (6.5)$$

Since the boundary $\Gamma_D^+ \cup \Sigma$ is smooth, the operator $\mathbf{K}^+ \mathbf{n}^+ \times$ is of order -1 . Our goal is to extend this result to the operator $\widetilde{T}_\Sigma \mathbb{A}_\Sigma^+$. We have

$$\begin{aligned} \widetilde{T}_\Sigma \mathbb{A}_\Sigma^+ &= (\chi_0 R^+ \mathbf{T}^+ P^+) (R^+ \mathbb{A}^+ P^+) \\ &= \chi_0 R^+ (\mathbf{T}^+ \mathbb{A}^+) P^+ + \chi_0 R^+ \mathbf{T}^+ (P^+ R^+ \mathbb{A}^+ - \mathbb{A}^+) P^+. \end{aligned}$$

It is clear to see that for $\mathbf{u} \in \mathbf{H}_{T,0}^s(\Sigma)$, $\mathbf{v} := (P^+R^+\mathbb{A}^+ - \mathbb{A}^+)P^+\mathbf{u} = (P^+R^+ - \text{Id})\mathbb{A}^+P^+\mathbf{u}$ vanishes on Σ . Since \mathbb{T}^+ is a convolution operator with a kernel $F(x, y)$ which is \mathcal{C}^∞ for $x \neq y$, we have $\chi_0R^+\mathbb{T}^+\mathbf{v} \in \mathbf{H}_T^\infty(\Sigma)$. This shows that the operator

$$D^+ = \chi_0R^+\mathbb{T}^+(P^+R^+\mathbb{A}^+ - \mathbb{A}^+)P^+$$

is of order $-\infty$. Note that we have used the fact that the support of χ_0 is included in the interior of Σ .

On the other hand, (6.5) leads to

$$\chi_0R^+(\mathbb{T}^+\mathbb{A}^+)P^+ = \chi_0R^+\left(\frac{1}{2}\text{Id} + \mathbb{K}^+\mathbf{n}^+\times\right)P^+ = \chi_0\frac{1}{2}\text{Id} + \chi_0R^+(\mathbb{K}^+\mathbf{n}^+\times)P^+.$$

Notice that $\chi_0\frac{1}{2}\text{Id} = \frac{1}{2}\text{Id}$ in $\mathbf{H}_{T,0}^s(\Sigma)$ and that $\chi_0R^+(\mathbb{K}^+\mathbf{n}^+\times)P^+$ is a pseudo-differential operator of order -1 in $\mathbf{H}_{T,0}^s(\Sigma)$, and is therefore compact. Remark that we have used the fact that $P^+(\mathbf{H}_{T,0}^s(\Sigma)) \subset \mathbf{H}_T^s(\partial\Omega^+)$.

Having the same results for the interior case, we obtain on $\mathbf{H}_{T,0}^s(\Sigma)$

$$\widetilde{\mathbb{T}}_\Sigma(\mathbb{A}_\Sigma^\pm) = \frac{1}{2}\text{Id} + \chi_0R^\pm(\mathbb{K}^\pm\mathbf{n}^\pm\times)P^\pm + D^\pm,$$

where $\chi_0R^\pm(\mathbb{K}^\pm\mathbf{n}^\pm\times)P^\pm$ and D^\pm are pseudo-differential operators of order -1 and $-\infty$ respectively. This concludes the proof. \square

In the real case, Γ_D is smooth and thus the boundaries $\Gamma_D^\pm \cup \Sigma$ are both lipschitzian but not of \mathcal{C}^1 regularity. Therefore the operator \mathbb{K}^\pm is no longer a compact operator in $\mathbf{H}_T^s(\Gamma_D^\pm \cup \Sigma)$. To study this case, a first possibility is to come back to the case of the theorem by distorting the boundaries $\Gamma_D^\pm \cup \Sigma$ in new boundaries $\widetilde{\Gamma}_D^\pm \cup \widetilde{\Sigma}$ such that these are \mathcal{C}^∞ (see FIG. 6.1, on the right), and by introducing the cut-off function χ_0 . The theoretical analysis of these two approximations (the change of boundaries and the multiplication by the smooth function χ_0) is not straightforward. A more direct approach would be to extend the theory of integral equations on surfaces with singularities. Such a theory was developed for bi-dimensional Helmholtz problems in [25], but its extension to three-dimensional Maxwell problems remains to be done.

7. Numerical Results

In this section, we first describe the numerical discretization chosen for the admittance operators \mathbb{A}_Σ^+ and \mathbb{A}_Σ^- . We then explain the discretization of the preconditioning by the operator \mathbb{T}_Σ of the equation (5.2), which couples the subdomains in our domain decomposition method.

We want to solve a numerical discretization of

$$(\mathbb{A}_\Sigma^+ + \mathbb{A}_\Sigma^-)\mathbf{u} = \mathbf{u}_0 \quad \text{on } \Sigma.$$

We recall that $\mathbb{A}_\Sigma^\pm\mathbf{v}_0 = R^\pm\mathbf{v}^\pm$ where \mathbf{v}^\pm is solution of the EFIE:

$$\mathbb{T}^\pm(\mathbf{v}^\pm) = \left(\frac{1}{2}\text{Id} + \mathbb{K}^\pm\mathbf{n}^\pm\times\right)(P^\pm\mathbf{v}_0).$$

To describe the action of the operator \mathbb{A}_Σ^\pm , one needs to discretize the EFIE.

We denote by Γ_h^\pm a family of triangulations of $\partial\Omega^\pm = \Gamma_D^\pm \cup \Sigma$ such that $\Sigma_h := \Gamma_h^+ \cap \Gamma_h^-$ is a family of triangulations of Σ . The space of H_{div} -conforming Rao-Wilton-Glisson finite elements on Σ_h is denoted by X_h , and we denote by $(\varphi_i)_{1 \leq i \leq N}$ its basis functions. Similarly, the notation X_h^\pm stand for the spaces of RWG finite elements on Γ_h^\pm , associated with basis functions $(\psi_i^\pm)_{1 \leq i \leq N^\pm}$, where $N^\pm > N$ and where we assume that $\forall i \leq N$, $\psi_i^\pm = \varphi_i$. These assumptions will allow us below to apply the preconditioner to a vector in the space X_h .

Let us describe the numerical computation of operator \mathbb{A}_Σ^\pm applied to a vector $\mathbf{v}_0 = \sum_{i=1}^N v_{0,i} \varphi_i$ of X_h . We first extend \mathbf{v}_0 to a vector \mathbf{v}_0^+ of X_h^+ defined by

$$\mathbf{v}_0^+ = P^+ \mathbf{v}_0 = \left(\sum_{i=1}^N v_{0,i} \varphi_i + \sum_{i=N+1}^{N^+} 0 \times \psi_i^+ \right) \in X_h^+,$$

and we denote by

$$V_0^+ = (v_{0,1}, \dots, v_{0,N}, 0, \dots, 0)^T$$

the vector of its components in the basis of X_h^+ .

Given an operator A and a space X of RWG functions associated with a triangulation T_0 , we denote by $[A]_X$ its Galerkin matrix for the L^2 -product using the basis functions $(\theta_i)_i$ of X , namely $([A]_X)_{ij} = \int_{T_0} A \theta_i \cdot \theta_j$. Consequently, the notation $[T^+]_{X_h^+}$ stands for the Galerkin matrix of the single layer operator defined on the triangulation X_h^+ .

The EFIE can be discretized as follows :

$$\text{Find } V^+ = (v_1, \dots, v_{N^+})^T \text{ such that } [T^+]_{X_h^+} V^+ = \left[\frac{1}{2} \text{Id} + \mathbf{K}^\pm \mathbf{n}^\pm \times \right]_{X_h^+} V_0^+,$$

where we have $\mathbf{v}^+ = \sum_{i=1}^{N^+} v_i \psi_i^+$. The vector $R^+ \mathbf{v}^+$ is finally given by $R^+ \mathbf{v}^+ = \sum_{i=1}^{N^+} v_i \varphi_i$.

From now on, we denote by $\langle \mathbb{A}_{X_h^\pm}^\pm \rangle$ the numerical computation of \mathbb{A}_Σ^\pm described above. Using the former finite elements, the equation (5.2) takes the form of the linear system

$$\left(\langle \mathbb{A}_{X_h^+}^+ \rangle + \langle \mathbb{A}_{X_h^-}^- \rangle \right) U = U_0,$$

where $U = (u_1, \dots, u_n)^T$ and $U_0 = (u_{0,1}, \dots, u_{0,n})^T$, with $\mathbf{u} = \sum_{i=1}^N u_i \varphi_i$ and $\mathbf{u}_0 = \sum_{i=1}^N u_{0,i} \varphi_i$.

To precondition the DDM, we have mathematically proposed a multiplication by the operator T_Σ . Numerically speaking, one wants to obtain a linear system close to the identity matrix. If we only multiplied the numerical vector by the matrix $[T_\Sigma]_{X_h}$, we would obtain a linear system close to the mass matrix $[\text{Id}]_{X_h}$. Therefore, we have to do a numerical multiplication by the matrix $[\text{Id}]_{X_h}^{-1} [T_\Sigma]_{X_h}$, in order to solve a system close to the identity matrix, and then better conditioned. As illustrated below, preconditioning the method with the Galerkin matrix $[T_\Sigma]_{X_h}$ is not enough to ensure an optimized convergence. One also needs to inverse the system by the mass matrix on the interface, which is realized through an iterative solution, of small numerical cost thanks to the sparsity of the matrix $[\text{Id}]_{X_h}$. This operation converts a vector whose coefficients are the L^2 -scalar products with the basis functions, into an amplitude vector (a vector whose coefficients are the coordinates in the basis functions).

We denote by DDM Y0 the original unpreconditioned equation related to the linear system $(\mathbb{A}_\Sigma^+ + \mathbb{A}_\Sigma^-)$,

$$\left(\langle \mathbb{A}_{X_h^+}^+ \rangle + \langle \mathbb{A}_{X_h^-}^- \rangle \right) U = U_0.$$

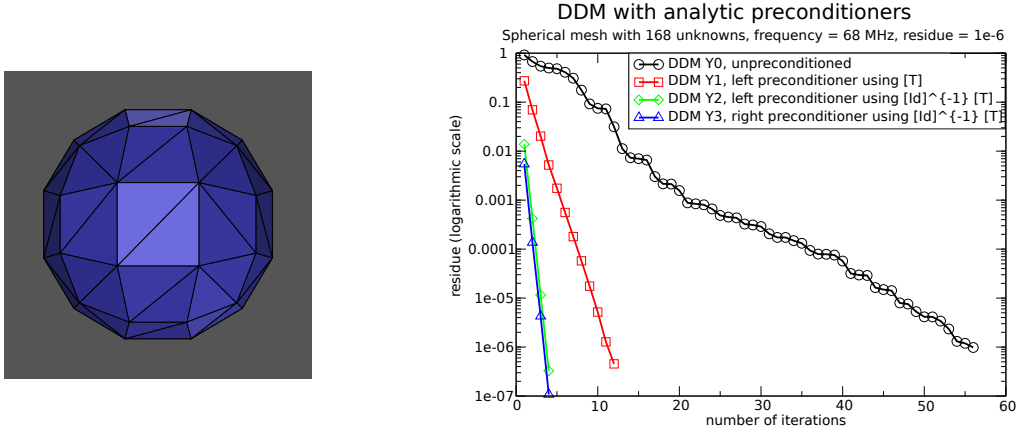


Fig. 7.1. Mesh (left) and convergence curves (right) to reach a residue of order 10^{-6} , for the artificial sphere at 68 MHz meshed with 168 DoF.

DDM Y1 is the equation with the left preconditioner being the Galerkin matrix of the single layer operator,

$$[\mathbf{T}_\Sigma]_{X_h} \left(\langle \mathbb{A}_{X_h^+}^+ \rangle + \langle \mathbb{A}_{X_h^-}^- \rangle \right) U = [\mathbf{T}_\Sigma]_{X_h} U_0.$$

DDM Y2 is the equation with the left preconditioner being the Galerkin matrix of the single layer operator, with an additional inversion by the mass matrix $[\mathbf{Id}]_{X_h}$,

$$[\mathbf{Id}]_{X_h}^{-1} [\mathbf{T}_\Sigma]_{X_h} \left(\langle \mathbb{A}_{X_h^+}^+ \rangle + \langle \mathbb{A}_{X_h^-}^- \rangle \right) U = [\mathbf{Id}]_{X_h}^{-1} [\mathbf{T}_\Sigma]_{X_h} U_0.$$

DDM Y3 is the equation with the right preconditioner being the Galerkin matrix of the single layer operator, and an inversion by the mass matrix $[\mathbf{Id}]_{X_h}$,

$$\left(\langle \mathbb{A}_{X_h^+}^+ \rangle + \langle \mathbb{A}_{X_h^-}^- \rangle \right) [\mathbf{Id}]_{X_h}^{-1} [\mathbf{T}_\Sigma]_{X_h} U = U_0.$$

Let us remark that we have to solve two kinds of linear systems. The first one is the linear system arising from the DDM itself. The second one is made of the systems which come from the discretization of the integral equations inside each subdomain. In order to solve both of them, we use the GMRES algorithm. Notice that the numerical scheme is a doubly nested iterative method.

7.1. Validation of the method

First of all, we consider the degenerate case where there is *no scattering object*. We denote by Σ the sphere centered at the origin and of diameter 1m, and we decompose \mathbb{R}^3 into two subdomains: the interior and the exterior of Σ . Notice that Lemma 6.1 applies to this situation. The sphere meshed with 168 DoF is shown on Fig. 7.1 (left), while the convergence curves are presented on Fig. 7.1 (right) at the frequency 68 MHz, and for the four equations above. Our first observation is that the unpreconditioned DDM Y0 converges really slowly in comparison with the three preconditioned DDM Y1, DDM Y2 and DDM Y3. DDM Y2 converges faster than DDM Y1, which lacks the inversion by the mass matrix. The results obtained with the

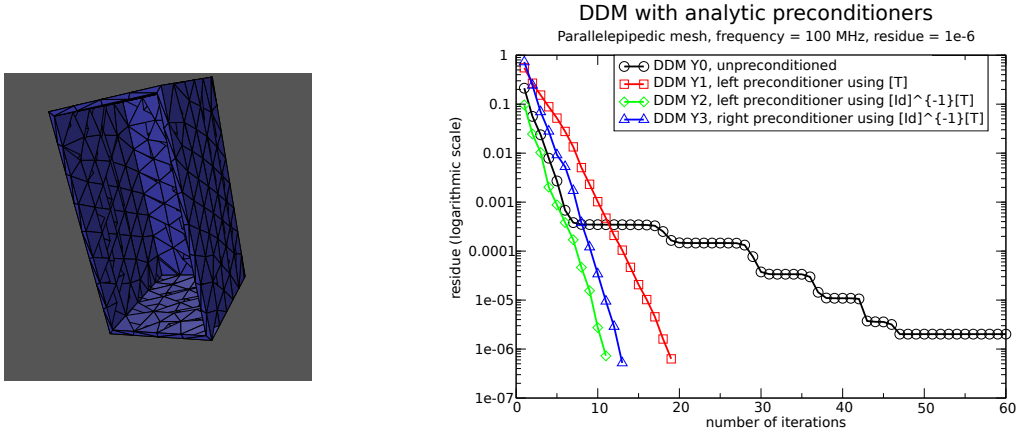


Fig. 7.2. Mesh (left) and convergence curves (right) to reach a residue of order 10^{-6} , for the parallelepipedic box at 100 MHz meshed with 102 DoF on the interface Σ .

right preconditioner (DDM Y3) are comparable with those of the left preconditioner (DDM Y2): both converge in as few as 4 iterations.

In the next experiment, there is a scattering object which contains a cavity. This is the original setting intended for our study. First, we present the case of an object whose shape is close to a parallelepipedic box which is open at one of its extremities (Fig. 7.2), and therefore exhibits a cavity. The interface Σ of this parallelepipedic box is a flat rectangle and is meshed with 102 DoF. For a residue of order 10^{-6} , DDM Y1, DDM Y2 and DDM Y3 converge respectively in 19, 13 and as few as 11 iterations, whereas the unpreconditioned method has not reached convergence after 1000 iterations.

On Fig. 7.3, we compare the radar cross section (RCS) obtained by the four methods to the one obtained with the integral equation EFIE on the global mesh, without any artificial interface. Although this case is quite simple, there is no artefact due to the method.

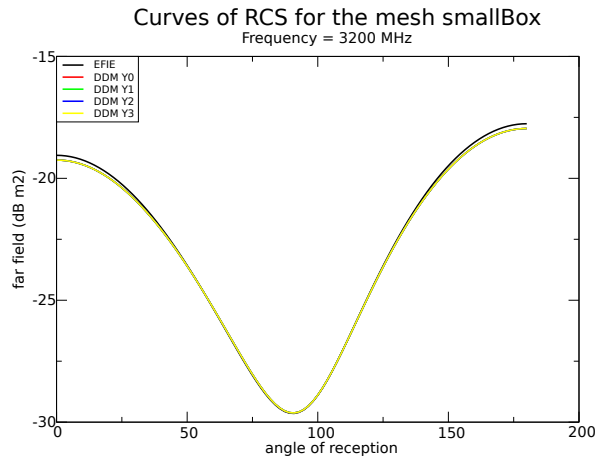


Fig. 7.3. Curves of RCS for the mesh smallBox at a frequency of 3200 MHz.

7.2. Reliability of the method with respect to the frequency

Our third experiment illustrates the influence of the frequency increase on the convergence rate, for the sphere again, but with a finer mesh of the spherical interface Σ , of 3072 DoF. We choose to compare only DDM Y0 (without preconditioner) with DDM Y2 (with the left preconditioner). The number of iterations to reach a residue of order 10^{-5} increases with the frequency for DDM Y0, whereas it remains stable (always 4 iterations) for DDM Y2 (Fig. 7.4 and Table 7.1). Consequently, the convergence rate is not altered by the increase of the frequency, as illustrated on Fig. 7.1, on the right, and on Fig. 7.4.

Table 7.1: Iterations count to reach a residue of order 10^{-5} depending on the frequency, for the sphere with 3072 DoF.

Frequency (MHz)	50	68	100	150	200	250	300	360
DDM Y0	96	101	104	160	181	189	199	216
DDM Y2	4	4	4	4	4	4	4	4

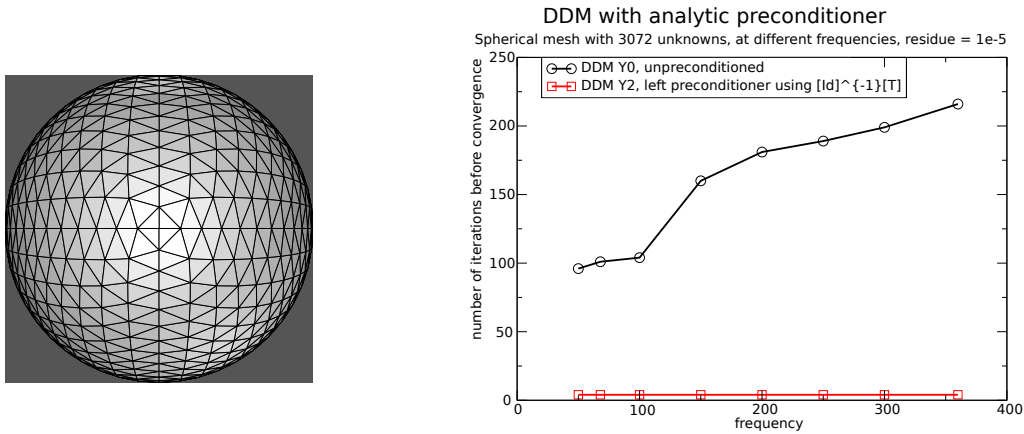


Fig. 7.4. Mesh (left) and influence of the frequency increase (right) on the number of iterations to reach a residue of order 10^{-5} , for the artificial sphere meshed with 3072 DoF.

7.3. Reliability of the method with respect to the number of unknowns

7.3.1. Artificial spheres (no real object)

We now refine the mesh of the sphere, passing from 3072 DoF to 5292 DoF. On this spherical mesh, at a frequency of 400 MHz, and to reach a residue of 10^{-4} , DDM Y2 converges in 28 iterations. The condition number of the linear system has obviously increased in comparison with

Table 7.2: For the algorithm DDM Y2, comparison between the number of iterations needed to reach a given residue at a given frequency, respectively for the spherical mesh with 3072 DoF and for the spherical mesh with 5292 DoF.

Equation	Frequency	Residue	Number of unknowns	Number of iterations
DDM Y2	360 MHz	10^{-5}	3072	4
DDM Y2	400 MHz	10^{-4}	5292	28

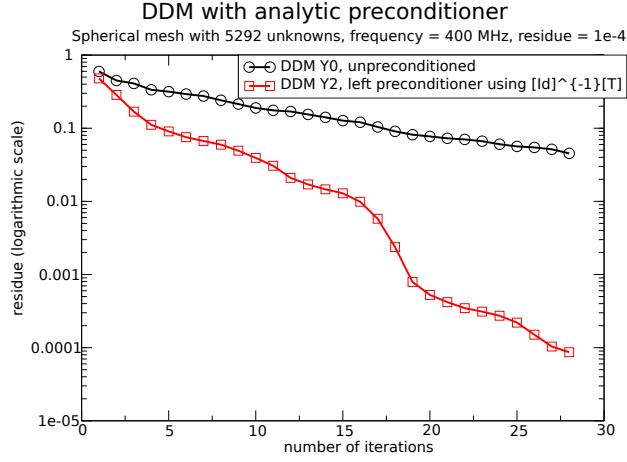


Fig. 7.5. Convergence curves to reach a residue of order 10^{-4} , for the spherical mesh with 5292 DoF, at a frequency of 400 MHz, respectively for DDM Y0 (unpreconditioned) and for DDM Y2 (with analytic preconditioner).

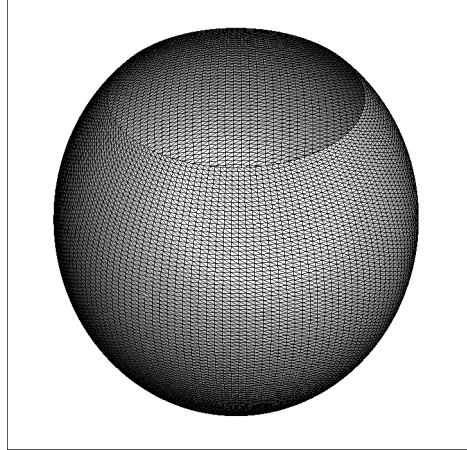


Fig. 7.6. Mesh (hollow35) of the hollow sphere of radius 1m. The interface (not represented) possesses 7420 DoF while the whole sphere has 44100 DoF.

the one of the former mesh (with 3072 DoF) (see Table 7.2), leading to a smaller convergence rate.

Nevertheless, looking at the convergence curves of the residues with respect to the iterations (Fig. 7.5), we observe that the unpreconditioned DDM Y0 converges much slower than DDM Y2. In particular, after 28 iterations, DDM Y0 has not reached a residue of $5 \cdot 10^{-2}$, whereas DDM Y2 has reached a residue of 10^{-4} . As a conclusion, this preconditioner remains very efficient for finer geometries.

7.3.2. Hollow spheres (real objects)

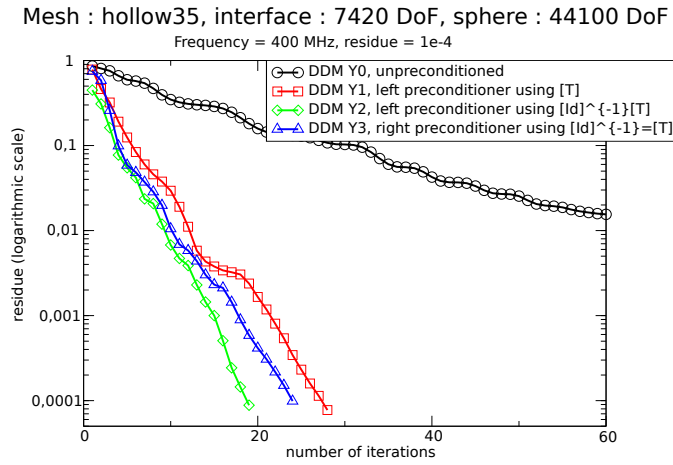
In this section, we illustrate the behavior of the algorithms (DDM Y0 to DDM Y3) when we refine the mesh of the scattering object. In that purpose, we consider a hollow sphere which

Table 7.3: Meshes of the considered hollow spheres.

Name of the mesh	Number of DoF on the interface (cap)	Number of DoF on the spherical mesh of both subdomains
hollow12	888	5184
hollow15	1380	8100
hollow20	2440	14400
hollow25	3800	22500
hollow30	5460	32400
hollow35	7420	44100

Table 7.4: Number of iterations to reach a residue of order 10^{-4} , at a constant frequency of 400 MHz, for the six meshes of the hollow sphere, for DDM Y0 (unpreconditioned) and DDM Y1, DDM Y2, DDM Y3 (with analytic preconditioners).

Equation Mesh	DDM Y0	DDM Y1	DDM Y2	DDM Y3
hollow12	152	27	17	18
hollow15	186	26	16	16
hollow20	> 60	27	16	19
hollow25	> 60	27	16	19
hollow30	> 60	28	17	22
hollow35	> 60	28	19	24

Fig. 7.7. Convergence curves to reach a residue of order 10^{-4} , for the mesh hollow35 of the hollow sphere, at a frequency of 400 MHz, respectively for DDM Y0 (unpreconditioned) and DDM Y1, DDM Y2, DDM Y3 (with analytic preconditioners).

constitutes the real scattering obstacle. The sphere is of radius 1 meter and is open for latitudes higher than 45 degrees, and is discretized with six different meshes of increasing precision (see Fig. 7.6 for the most refined mesh).

The artificial interface needed for the DDM algorithm is chosen to be the missing cap of the sphere. Therefore, the interior and exterior problems consist in solving Maxwell equations inside and outside the sphere, respectively. They exchange data on the cap while, on the rest of

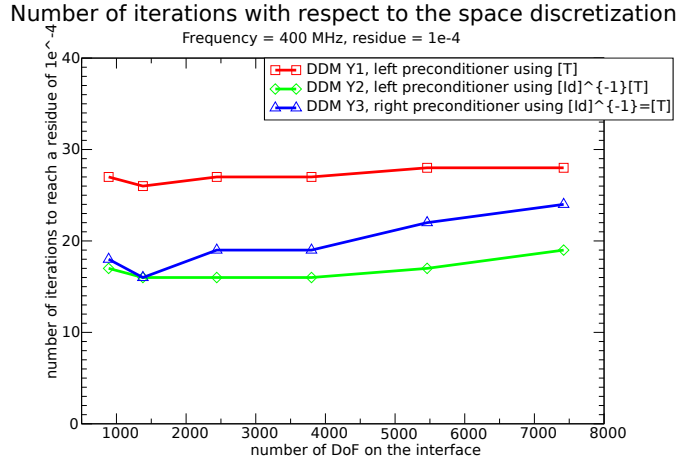


Fig. 7.8. Comparison of the number of iterations for the preconditioned equations DDM Y1, DDM Y2, DDM Y3, to reach a residue of 10^{-4} , at a constant frequency of 400 MHz. For each curve, each point corresponds to one of the different meshes that we have considered, namely with 888, 1380, 2440, 3800, 5460 and 7420 DoF on the interface.

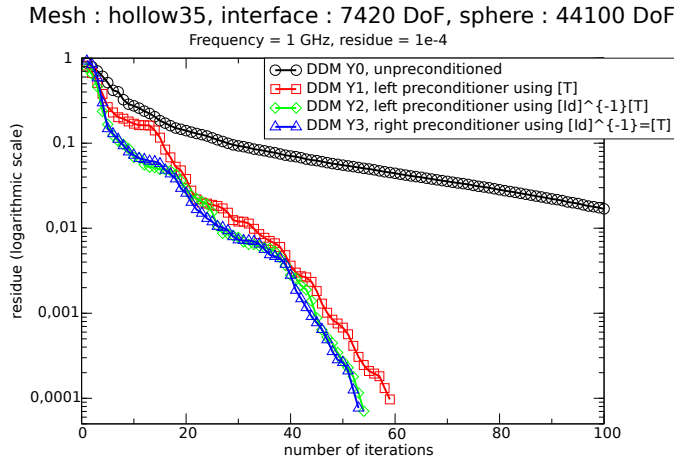


Fig. 7.9. Convergence curves to reach a residue of order 10^{-4} , for the mesh hollow35 of the hollow sphere, whose interface is meshed with 7420 DoF, at a frequency of 1 GHz, respectively for DDM Y0 (unpreconditioned) and DDM Y1, DDM Y2, DDM Y3 (with analytic preconditioners).

the sphere, we have a Dirichlet type boundary condition. We give in Table 7.3 the number of unknowns respectively on the interface and on the whole sphere, for each considered mesh. Due to the size of the meshes, and contrarily to what has been done so far, we use a fast multipole method (FMM) to compress all involved linear systems.

We show in Fig. 7.7 the convergence rates for the four methods DDM Y0 to DDM Y3 in the finest case (hollow35), for a frequency of 400 MHz. Once again, the unpreconditioned DDM Y0 converges much slower than the three other preconditioned equations (DDM Y1, DDM Y2,

Table 7.5: Number of iterations to reach a residue of order 10^{-4} , at a frequency of 1 GHz, for the mesh hollow35, whose interface is meshed with 7420 DoF, for DDM Y0 (unpreconditioned) and DDM Y1, DDM Y2, DDM Y3 (with analytic preconditioners).

Equation Mesh	DDM Y0	DDM Y1	DDM Y2	DDM Y3
hollow35	> 100	59	54	53

DDM Y3). For instance, DDM Y1 (resp. DDM Y2, DDM Y3) reaches a residue of 10^{-4} in 28 iterations (resp. 19, 24 iterations), whereas DDM Y0 has not yet reached a residue of 10^{-2} in 60 iterations. The explicit numbers of iterations for all meshes are provided in Table 7.4.

Increasing the frequency of the problem to 1 GHz, only for the finest mesh (hollow35), does not deteriorate the method that much. Indeed, we show in Fig. 7.9 and Table 7.5 that the three preconditioned methods DDM Y1, DDM Y2, DDM Y3 remain very competitive in comparison with DDM Y0.

8. Conclusion

We have proposed a domain decomposition method associated with an efficient preconditioner, based on the restriction of the single layer operator on the interface between the subdomains. In each subdomain, the EFIE is solved at each iteration. The numerical results illustrate the very good behavior of the resulting preconditioned algorithm, which converges much faster than without preconditioning.

Nevertheless, although the proposed method seems very encouraging, several difficulties need still to be overcome in order to make the method usable in real applications. First, the present formulation is restricted to the case where the EFIE is solved in each subdomain. Clearly, there is an obvious obstruction for resonant frequencies. In order to circumvent this issue, we have to generalize the approach for other formulations (e.g., CFIE, or the recent very efficient GCSIE methods [1, 2]).

Another improvement direction consists in changing the coupling condition on the surface Σ between the subdomains. For instance, when one takes impedant coupling boundary conditions, it is well known that the underlying problems are well-posed for any frequency [8]. Again, the GCSIE formalism, originally developed for metallic problems, has recently been extended to impedant ones in [23] and [27], and could prove to be very efficient.

We plan to investigate those issues and even combinations of them in the foreseeing future.

Acknowledgements. We would like to address special thanks to Jean-Marie Mirebeau for helpful suggestions.

References

- [1] F. Alouges, S. Borel, and D.P. Levadoux, A stable well-conditioned integral equation for electromagnetism scattering, *J. Comp. Appl. Math.*, **204** (2007), 440–451.
- [2] F. Alouges and D.P. Levadoux, Well-conditioned integral equations for high-frequency scattering problems, *8th International Conference on Mathematical and Numerical Aspects of Waves*, Reading, UK (2007), 47–51.

- [3] X. Antoine and Y. Boubendir, An integral preconditioner for solving the two-dimensional scattering transmission problem using integral equations, *International Journal of Computer Mathematics*, **85**:(10) (2008), 1473–1490.
- [4] N. Balin, A. Bendali, and F. Collino, Domain decomposition and additive Schwarz techniques in the solution of a TE model of the scattering by an electrically deep cavity, *In Selected papers of the 15th International Conference on Domain Decomposition Methods in Science and Engineering, Berlin, Germany, July 21-25 2003 Eds. R. Kornhuber, R. Hoppe, J. Périaux, O. Pironneau and J. Xu, Springer* (2005), 149–156.
- [5] N. Balin, A. Bendali, M. Fares, F. Millot, and N. Zerbib, Some recent applications of substructuring and domain decomposition techniques to radiation and scattering of time-harmonic electromagnetic waves, *CERFACS report TR/EMC/05/80*, **7** (2005), 474–485.
- [6] S. Borel, D.P. Levadoux, and F. Alouges, A new well-conditioned integral formulation for Maxwell equations in three-dimensions, *IEEE Trans. Antennas Propag.*, **53**:(9) (2005), 2995–3004.
- [7] A.J. Burton and G.F. Miller, The application of integral equation methods to the numerical solution of the exterior boundary-value problems, *Proc. Roy. Soc. Lond. A.*, **323** (1971), 201–210.
- [8] F. Cakoni, D. Colton, and P. Monk, The electromagnetic inverse-scattering problem for partially coated lipschitz domains, *Proc. Royal. Soc. Edinburgh*, **134A** (2004), 661–682.
- [9] J. Chazarain and A. Piriou, Introduction à la Théorie des Équations aux Dérivées Partielles Linéaires, Gauthier-Villars 1981.
- [10] S.H. Christiansen and J.-C. Nédélec, A preconditioner for the electric field integral equation based on Calderón formulas, *SIAM J. Numer. Anal.*, **40**:(3) (2002), 1100–1135.
- [11] F. Collino, S. Ghanemi, and P. Joly, Domain decomposition method for harmonic wave propagation: a general presentation, *Comp. Meth. Appl. Mech. Engrn.*, **184** (2000), 171–211.
- [12] F. Collino and F. Millot, Mise en place d’un préconditionneur analytique appliqué à un problème d’électromagnétisme, *Technical Report TR/EMC/02/122, CERFACS* 2003.
- [13] D. Colton and R. Kress, Integral Equation Methods in Scattering Theory, John Wiley & Sons 1983.
- [14] M. Darbas, Generalized combined field integral equations for the iterative solution of the three-dimensional maxwell equations, *Applied Mathematics Letters*, **19**:(8) (2006), 834–839.
- [15] B. Després, Domain decomposition method and the Helmholtz problem, *Mathematical and numerical aspects of wave propagation phenomena*, SIAM, Philadelphia (1991), 44–52.
- [16] B. Després, Méthodes de décomposition de domaine pour les problèmes de propagation d’ondes en régime ordinaire, PhD thesis, Université Paris IX Dauphine 1991.
- [17] V. Dolean, M.J. Gander, and L. Gerardo-Giorda, Optimized schwarz methods for maxwell’s equations, *SIAM Journal on Scientific Computing*, **31**:(3) (2009), 2193–2213.
- [18] M.J. Gander, L. Halpern, and F. Magoules, An optimized schwarz method with two-sided robin transmission conditions for the helmholtz equation, *Int. J. for Num. Meth. in Fluids*, **55**:(2) (2007), 163–175.
- [19] M.J. Gander, L. Halpern, and F. Nataf, Optimal schwarz waveform relaxation for the one dimensional wave equation, *SIAM Journal on Numerical Analysis*, **41**:(5) (2003), 1643–1681.
- [20] R. Hiptmair and P. Meury, Stabilized FEM-BEM coupling for Helmholtz transmission problems, *SIAM J. Numer. Anal.*, **44** (2006), 2107–2130.
- [21] R. Hiptmair and P. Meury, Stabilized FEM-BEM coupling for Maxwell transmission problems, In H. Ammari, editor, *Modelling and Computations in Electromagnetics*, Lecture Notes in Computational Science and Engineering, Springer, Berlin, **59** (2007), 1–39.
- [22] D.P. Levadoux, Some preconditioners for the CFIE equation of electromagnetism, *Math. Meth. Appl. Sci.*, **17** (2008), 2015–2028.
- [23] D.P. Levadoux, F. Millot, and S. Pernet, New trends in the preconditioning of integral equations of electromagnetism, *Springer-Verlag Berlin Heidelberg, Scientific Computing in Electrical Engineering SCEE 2008 by Janne Roos, Luis R. J. Costa (Mathematics in industry 14)* (2010),

- 383–394.
- [24] K.M. Mitzner, Numerical solution of the exterior scattering problem at eigenfrequencies of the interior problem, *Int. Scientific Radio Union Meeting*, Boston, Mass. Mar. 1968.
 - [25] S. Molko-Daugas, Prise en compte des singularités géométriques dans le préconditionnement d'équations intégrales pour le problème de Helmholtz, PhD thesis, Université Paris XI, France 2010.
 - [26] J.-C. Nedelec, Acoustic and Electromagnetic Equations, integral representations for harmonic problems, Springer 2001.
 - [27] S. Pernet, A well-conditioned integral equation for iterative solution of scattering problems with a variable Leontovich boundary condition, *ESAIM: Mathematical Modelling and Numerical Analysis*, **44** (July 2010), 781–801.
 - [28] V. Rokhlin, Diagonal form of translation operators for the Helmholtz equation in three dimensions, *Appl. Comput. Harmon. Anal.*, **1** (1993), 82–93.
 - [29] J. Simon, Extension de méthodes multipôles rapides: résolution pour des seconds membres multiples et application aux objets diélectriques, PhD thesis, Université de Versailles Saint-Quentin-en-Yvelines, France 2003.
 - [30] O. Steinbach and W.L. Wendland. The construction of some efficient preconditioners in the boundary element method, *Adv. Comput. Math.*, **9**:(1–2) (1998), 191–216.
 - [31] W. McLean, T. Tran, A preconditioning strategy for boundary element galerkin methods, *Numer. Methods for Partial Differential Equations*, **13** (1997), 283–301.